

3,6-Disubstituted Coumarins as Mechanism-Based Inhibitors of Thrombin and Factor Xa

Raphaël Frédérick,^{†,‡} Séverine Robert,^{†,‡} Caroline Charlier,[§] Jérôme de Ruyck,[§] Johan Wouters,[§] Bernard Pirotte,[#] Bernard Masereel,[†] and Lionel Pochet^{*,†}

Department of Pharmacy and CBS Laboratory, University of Namur, FUNDP, 61, Rue de Bruxelles, B-5000 Namur, Belgium, and Natural and Synthetic Drug Research Centre, University of Liège, ULG, 1, Avenue de l'Hôpital bât B36, Tour 4, B-4000 Liège, Belgium

Received May 11, 2005

In this work, coumarins were screened on thrombin (THR) and factor Xa (FXa), two of the most promising targets for the development of anticoagulant drugs. This allowed us to highlight compound **30**, characterized by a 2,5-dichlorophenyl ester in the 3-position and a chloromethyl moiety in the 6-position, as a very potent THR inhibitor ($k_i/K_i = 37\,000\text{ M}^{-1}\text{ s}^{-1}$). Moreover, this compound exhibits good selectivity over FXa (168-fold) and trypsin (54-fold). The mechanism of inactivation was investigated in this series and significantly differs from that previously observed with α -chymotrypsin. Indeed, the addition of hydrazine on the THR–inhibitor complex promotes a partial induced THR reactivation. This reactivation, confirmed by LC/MS, showed the resurgence of the native THR and a new dihydrazide complex. Docking experiments were then efficiently used to explain the trends observed in the enzymatic assays as well as to corroborate the postulated inhibition mechanism. Finally, the cell permeability of our derivatives was estimated using a computational approach.

Introduction

Thrombin (THR) and factor Xa (FXa) constitute important trypsin-like serine proteases involved in the coagulation cascade. THR plays a key role in thrombosis and hemostasis.^{1–3} Indeed, as the terminal enzyme of the coagulation cascade, THR is directly responsible for the conversion of glycoprotein fibrinogen to fibrin.^{4–7} Moreover, besides the cleavage of fibrinogen, THR amplifies its own generation by feedback activation of factors V, VIII, and IX and stimulates platelet activation. In contrast, when bound to thrombomodulin, it causes a feedback inhibition of the coagulation cascade by activation of protein C. This, in turn, inactivates factors Va and VIIIa by proteolytic degradation. Because of its importance in thrombosis, THR has been recognized early as a major target for the development of inhibitors.

FXa is the point of convergence of the intrinsic and extrinsic pathways. In association with phospholipids, factor Va, and calcium, it forms the prothrombinase complex and catalyzes the conversion of prothrombin in THR. Therefore, FXa constitutes another key target for the development of anticoagulants, which might be even more efficient than THR inhibition in interrupting the blood coagulation cascade.^{8–10}

Current anticoagulant therapies clinically used in the treatment of acute and chronic thrombosis involve the use of (i) heparins and related compounds¹¹ acting through activation of antithrombin III, a glycoprotein that nonselectively inhibits THR, FXa, and factor IXa,

and (ii) 4-OH-coumarins, as warfarin and acenocoumarol,¹² which inhibit the hepatic synthesis of vitamin-K dependent proteins including THR and FXa. Owing to their indirect and nonselective mechanism of action, both classes of anticoagulants require careful clinical monitoring. Moreover, they are often associated with numerous drug interactions and side effects. Therefore, many efforts have been devoted finding novel classes of low molecular weight direct THR and FXa inhibitors.^{13,14} These could be safer and more selective than current therapies.

To date, two types of low molecular weight active site directed THR inhibitors have been developed and classified according to their mechanism of action. The first class inhibits THR in a noncovalent manner. These compounds fill the enzyme active site and are stabilized within the S1–S3 specificity pockets through hydrogen-bonding, hydrophobic, and electrostatic interactions. Representative compounds of this class include argatroban,¹⁵ NAPAP,¹⁶ inogatran,¹⁷ melagatran,¹⁸ and napsagatran.¹⁹ The second class consists of inhibitors that covalently interact with Ser195 of the catalytic triad. In addition, these compounds usually possess an electrophilic center such as a chloromethyl ketone as observed in PPACK,²⁰ a C-terminal aldehyde,²¹ a fluoromethyl ketone,²² a α -ketoester,²³ an amide,²⁴ a phosphonate,²⁵ a phosphonite,²⁵ or a boronic acid function.²⁶ A large variety of small molecular weight active site directed FXa inhibitors, distributed in two groups, have also emerged in the literature: (i) covalent inhibitors derived from the peptide substrate^{27,28} and (ii) noncovalent inhibitors such as the bis-arylamidine DX-9065a²⁹ or the bis-amidine ZK-807834.³⁰ Whatever the targeted enzyme, many of these inhibitors have a basic P1 side chain to facilitate the formation of a salt-bridge with Asp189 located at the bottom of the S1 pocket.

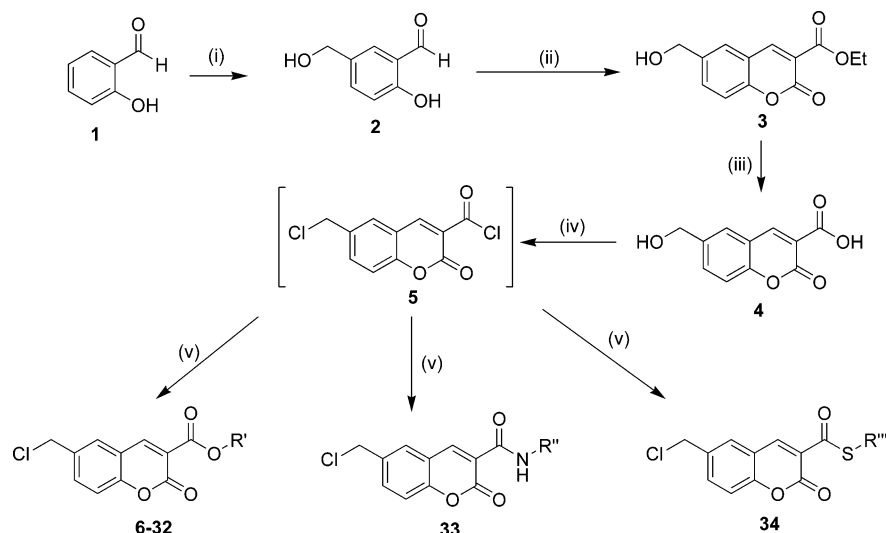
* To whom correspondence should be addressed. Phone: +32 (0)81 72 42 92. Fax: +32 (0)81 72 42 99. E-mail: lionel.pochet@fundp.ac.be.

[†] Department of Pharmacy, University of Namur.

[‡] These authors equally contributed to this work.

[§] University of Liège.

[#] CBS Laboratory, University of Namur.

Scheme 1. Synthesis of the Esters **6–32**, Amide **33**, and Thioester Derivatives **34**^a

^a Reagents and conditions: (i) HCHO, HCl, 80 °C, 20 min; (ii) diethyl malonate, piperidine, AcOH, EtOH, reflux, 17 h; (iii) HCl (3 N), EtOH, reflux, 3 h; (iv) SOCl₂, reflux, 3 h; (v) R'OH or R''NH₂, or R'''SH, C₅H₅N, dioxane, 25 °C, 1 h 30 min.

Nevertheless, this basic moiety is usually responsible for poor bioavailability. So several laboratories aimed to develop less basic, low molecular weight, selective inhibitors of THR and FXa.^{31–35}

Previously, we reported that particular coumarins were powerful inhibitors of α -chymotrypsin (α -CT) and human leukocyte elastase (HLE), two serine proteases implicated in numerous biological processes such as digestion (α -CT) and phagocytosis (HLE).^{36–39} These compounds are characterized by an alkyl or an aryl moiety linked to the heterocycle by an ester, a thioester, an amide, or a ketone function in the 3-position and an electrophilic chloromethyl group in the 6-position. They were found to act as mechanism-based inhibitors. Interestingly, THR and FXa share the same catalytic mechanism with α -CT and HLE. Moreover, it was shown that a proper pharmacomodulation of isocoumarins, initially developed as HLE inhibitors, could afford selective THR inhibitors.^{40,41} Therefore, in this paper, we have evaluated the efficiency of 3,6-disubstituted coumarins, characterized by a nonbasic side chain, as potent THR and FXa inhibitors. For this purpose, new compounds were synthesized. The postulated inhibition mechanism toward THR was investigated using reactivation and mass spectrometry experiments (LC/MS), and compared with that of α -CT. Molecular docking was performed on relevant compounds to corroborate our hypothesis and to explain the trends observed in the enzymatic assays. Finally, we have estimated the cell permeability of some derivatives using a computational approach. On the basis of the results as a whole, it was shown that according to the nature of the substituent in the 3-position, coumarins could act as very potent THR inhibitors, with a partially induced reactivation profile and good cell permeation.

Chemistry

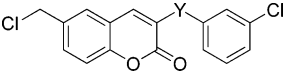
6-Chloromethylcoumarins **6–34** were obtained using the strategy depicted in Scheme 1.^{36–38} 5-Hydroxymethylsalicylaldehyde **2** was achieved by reaction of salicylaldehyde **1** with formaldehyde. Then the condensation of **2** with diethyl malonate through a Knoevena-

Table 1. In Vitro THR and FXa Inhibitory Potency of Aryl Esters

compd	R	residual activity (%)	
		THR	FXa
6	phenyl	60 ± 9	59 ± 18
7	benzyl	95 ± 5	110 ± 6
8	2-pyridyl	100 ± 5	89 ± 15
9	3-pyridyl	113 ± 11	114 ± 15
10	1-naphthyl	115 ± 18	109 ± 12
11	2-naphthyl	109 ± 14	113 ± 5
12	6-quinolyl	98 ± 10	125 ± 7
13	8-quinolyl	107 ± 14	114 ± 11
14	<i>o</i> -chlorophenyl	78 ± 8	134 ± 9
15	<i>m</i> -chlorophenyl	10 ± 2	29 ± 3
16	<i>p</i> -chlorophenyl	107 ± 12	102 ± 6
17	<i>o</i> -iodophenyl	59 ± 13	92 ± 13
18	<i>m</i> -iodophenyl	27 ± 8	73 ± 9
19	<i>p</i> -iodophenyl	99 ± 10	80 ± 8
20	<i>o</i> -toluyl	79 ± 3	103 ± 12
21	<i>m</i> -toluyl	35 ± 3	78 ± 16
22	<i>p</i> -toluyl	111 ± 20	72 ± 8
23	<i>m</i> -fluorophenyl	24 ± 6	61 ± 16
24	<i>m</i> -bromophenyl	8 ± 3	33 ± 3
25	<i>m</i> -nitrophenyl	80 ± 2	124 ± 32
26	<i>m</i> -methoxyphenyl	66 ± 4	108 ± 21
27	<i>m</i> -trifluoromethylphenyl	66 ± 21	134 ± 13
28	3-chloro-5-methoxyphenyl	103 ± 5	126 ± 28
29	2,3-dichlorophenyl	100 ± 12	125 ± 22
30	2,5-dichlorophenyl	1.0 ± 0.1	39 ± 6
31	2,6-dichlorophenyl	101 ± 11	109 ± 21
32	3,5-dichlorophenyl	102 ± 10	73 ± 8

gel type reaction gave the 6-hydroxymethyl-2-oxo-2H-1-benzopyran-3-carboxylic acid ethyl ester **3**, which was further hydrolyzed to obtain **4**. Reaction of **4** with thionyl chloride yielded the acyl chloride **5**, which reacted with the required alcohol, amine, or thiol to give the esters **6–32** (Table 1), the amide **33** (Table 2), and the thioester **34** (Table 2).

The synthesis of ketones **40–41** followed the strategy illustrated in Scheme 2. According to this pathway, we prepared the β -ketoester **37** by reaction of the acyl chloride **36** of 3-chlorophenylacetic acid **35** with Mel-

Table 2. In Vitro THR and FXa Inhibitory Potency of Thioester, Amide, and Ketone Derivatives


compd	Y	residual activity (%)	
		THR	FXa
15	COO	10 ± 2	29 ± 3
33	CONH	97 ± 2	89 ± 7
34	COS	107 ± 12	60 ± 7
40	CO	100 ± 15	83 ± 2
41	COCH ₂	77 ± 5	77 ± 3

drum's acid followed by decarboxylation in refluxing ethanol. Then the ketone derivatives **38–39** were obtained by condensation of **2** with **37** or commercially available 3-(3-chlorophenyl)-3-oxopropionic acid ethyl ester. Derivative **40** was achieved through the reaction of **38** with refluxing thionyl chloride. For the conversion of alcohol **39** into the alkyl halide **41**, we performed the one-pot procedure described by Iranpoor.⁴² This method, which employs the PPh₃/DDQ/(*n*-hexyl)₄NCl system, allowed us to obtain the chloromethyl **41**.

Derivatives **42–44** (Table 3) were synthesized according to the strategy presented in Scheme 1 using the corresponding commercially available salicylaldehyde and β -ketoester.

Results and Discussion

In earlier studies, we found that the most potent inhibitors of α -CT and HLE possessed an aryl ester substituent in the 3-position.^{36,38} Therefore, we decided to evaluate the potency of various aryl derivatives (**6–32**) against human THR and FXa.

Enzyme Inhibition. To evaluate their inhibitory potency toward THR and FXa, a screening test was developed. In this test, the proteolytic activity is measured 10 min after incubation with the inhibitor at 2 and 5 μ M for THR and FXa, respectively. The results, displayed in Table 1, are expressed as the percentage of enzyme residual activity.

The phenyl ester **6** is a moderately efficient THR and FXa inhibitor. The replacement of the phenyl ring by a benzyl **7**, a pyridyl (**8**, **9**), or a bulkier aryl group such as a naphthyl (**10**, **11**) or a quinolyl group (**12**, **13**) leads to a complete loss of inhibitory potency on both proteases. The influence of substitution on the phenyl ring was then investigated. As observed with HLE and α -CT, the type and the position of the substituent strongly influence THR and FXa inhibitory potency. Indeed, whatever their nature, ortho (**14**, **17**, **20**) and para substituents (**16**, **19**, **22**) seem to be always unfavorable. The most active compounds, on both proteases, possess a halogen group in the meta position (**15**, **18**, **23**, **24**). Molecules possessing a nitro **25**, a methoxy **26**, or a trifluoromethyl moiety **27** in the meta position only moderately inhibit THR, whereas a complete loss of FXa inhibitory potency is observed. Among the dichlorophenyl derivatives (**29–32**), it should be noted that only the 2,5-dichlorophenyl **30** is strongly efficient on THR. This latter, which fairly inhibits FXa at 5 μ M, was found to be the most potent THR inhibitor in this series (1.0 ± 0.1% of THR residual activity at 2 μ M).

The influence of the link between the coumarin ring and the phenyl side chain in the 3-position was also

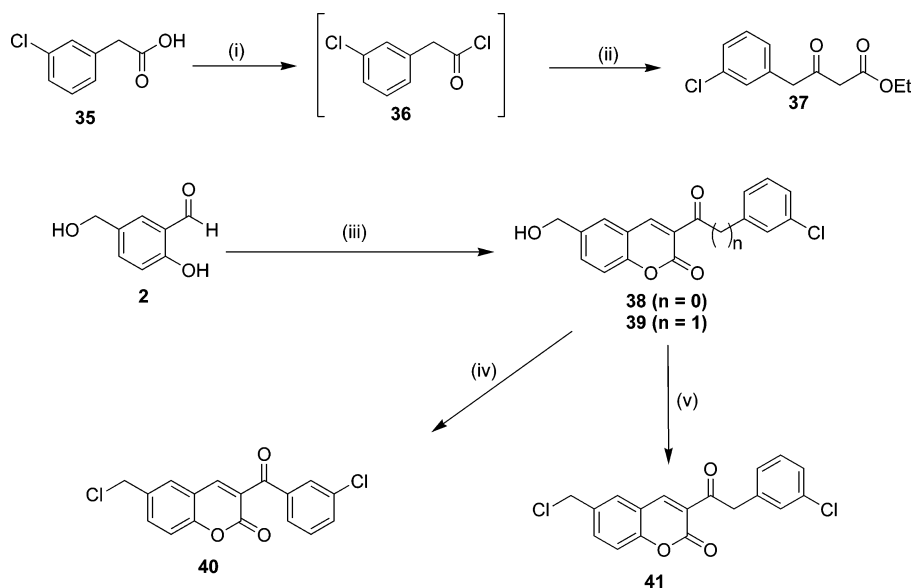
investigated (Table 2). For this purpose, we synthesized compounds **40** and **41** characterized by a ketone link between the coumarin ring and the aromatic side chain. The inhibitory potency of these molecules was compared with the corresponding ester **15**, amide **33**, and thioester **34**. In each case, the replacement of the ester function strongly decreases the inhibitory potency toward THR and FXa. As observed for α -CT and HLE, the amide link suppresses the inhibitory potency. We previously showed that this amide function highly stabilizes an anti conformation in which both carbonyl groups point in opposite directions.⁴³ Therefore, the lack of inhibitory potency of the amide derivative **33** could be associated with a poor recognition of this conformation in THR and FXa binding sites. Surprisingly, the thioester **34** is found to be inactive on THR at 2 μ M and moderately active on FXa at 5 μ M, whereas this compound was as potent as the ester on α -CT.³⁸ The new synthesized ketones (**40**, **41**) are less active than the corresponding ester **15**. The ketone **40** is inactive at 2 μ M on THR and not very active on FXa at 5 μ M, while the methylene ketone **41** is fairly active on both proteases.

We also considered the influence of the moiety introduced in the 6-position (Table 3). The removal (**43**) or the substitution of a methyl (**42**) or an acetoxymethyl (**44**) moiety for the chloromethyl group (**15**) strongly decreases the inhibitory potency on both proteases. These results suggest that the chloromethyl function plays a key role in the inhibition process, as postulated in the inhibition mechanism proposed for other serine proteases.⁴⁴ From earlier work, it appeared that the importance of this moiety depends on the targeted enzyme: the replacement of the chloromethyl leads to a complete loss of the activity toward α -CT, whereas with HLE, the activity is preserved.³⁷

In conclusion, similar structure–activity relationships have been drawn from both enzymes. Although the compounds are generally more potent on THR than on FXa, the substitution of the aryl moiety in the 3-position by a halide in the meta or in the 2,5-position improved the inhibitory potency on both enzymes. In each case, the replacement of the ester link between the coumarin ring and the side chain usually decreases the activity of the compounds. And finally, the removal or the substitution of the chloromethyl in the 6-position always lead to a drastic loss in inactivator potential.

Inactivation Kinetics and Selectivity. For the most active compounds, we determined the k_i/K_i ratio, which is the index of the inhibitory potency for mechanism-based inhibitors.⁴⁵ The kinetic parameters k_i and K_i were determined using either the progress curve or the preincubation method.³⁷ In the progress curve method, the inhibitor competes with a chromogenic substrate to bind the enzyme. In the preincubation method, in contrast, the enzyme and the inhibitor are incubated together before the determination of the remaining activity at regular time intervals.

For THR, the most potent inhibitor was the 2,5-dichlorophenyl ester **30** with a k_i/K_i ratio of 37 000 M^{−1} s^{−1} (Table 4). The THR inhibitory potency of the *m*-bromo **24** (k_i/K_i = 10 540 M^{−1} s^{−1}) and *m*-chloro **15** (k_i/K_i = 7720 M^{−1} s^{−1}) derivatives were in the same range, whereas the *m*-fluoro **23** (k_i/K_i = 2970 M^{−1} s^{−1}) and *m*-iodo **18** (k_i/K_i = 1210 M^{−1} s^{−1}) derivatives were

Scheme 2. Synthesis of the Ketone Derivatives **40** and **41**^a

^a Reagents and conditions: (i) SOCl_2 , reflux, 1 h; (ii) (a) Meldrum's acid, pyridine, CH_2Cl_2 , 0 °C to room temp, 2 h; (b) EtOH, reflux, 3 h; (iii) corresponding β -ketoester, piperidine, AcOH, EtOH, reflux, 17 h; (iv) SOCl_2 , reflux, 2 h; (v) PPh_3 , DDQ, $(n\text{-hexyl})_4\text{NCl}$, CH_2Cl_2 , room temp, 5 min.

Table 3. In Vitro THR and FXa Inhibitory Potency of 6-Substituted Ester Derivatives

compd	X	residual activity (%)	
		THR	FXa
15	CH_2Cl	10 ± 2	29 ± 3
42	CH_3	70 ± 4	61 ± 3
43	H	107 ± 7	77 ± 7
44	$\text{CH}_2\text{OCOCH}_3$	91 ± 15	82 ± 7

less active. Compound **30** also displayed a good selectivity profile because its selectivity ratio of THR to FXa and trypsin (TRY) was 168 and 54, respectively.

For compounds **15**, **24**, and **30**, the weak FXa inhibition associated with the poor solubility of coumarins did not allow us to use the progress curve method for the determination of the kinetic parameters. Therefore, the preincubation method was used to determine the k_i/K_i ratio expressed as $k_{\text{obs}}/[\text{I}]$. A good correlation between these two methods was obtained because the k_i/K_i and $k_{\text{obs}}/[\text{I}]$ ratios on FXa inhibition for **15** were 655 and 620 $\text{M}^{-1} \text{s}^{-1}$, respectively. The herein obtained results confirmed that these coumarins possessed only a weak FXa inhibitory potency. The best FXa inhibitors **15** ($k_{\text{obs}}/[\text{I}]$ of 620 $\text{M}^{-1} \text{s}^{-1}$) appeared to be also a good THR inhibitor ($k_i/K_i = 7720 \text{ M}^{-1} \text{s}^{-1}$).

For comparison purposes, we determined IC_{50} values on THR for the best derivative **30** in this series and for argatroban, a well-known THR inhibitor.¹⁵ IC_{50} values were 103 ± 32 and $331 \pm 22 \text{ nM}$ for **30** and argatroban, respectively. According to the Cheng–Prusoff equation,⁴⁶ we estimated a K_i value for argatroban of 13 nM, which is in agreement with the published value.¹⁵ According to this experiment, **30** seemed to be at least as potent as argatroban. Nevertheless, since the type of inhibition of these two derivatives is different (mech-

anism-based inhibitor for **30** vs competitive inhibitor for argatroban), the comparison should be analyzed with care.

Reactivation. The reversible or irreversible character of the THR inhibition by compounds **15** and **30** was analyzed. Previously, we showed that 6-chloromethylcoumarins irreversibly inhibited $\alpha\text{-CT}$.⁴⁴ Conversely, reactivation of HLE arose, sped up by hydroxylamine.³⁷ In the case of THR inhibited by **15** or **30** (Figure 1), we studied the spontaneous reactivation during 2 days. Only a poor recovery of activity, from 10% to 35% for **15** (Figure 1a) and from 1% to 11% for **30** (Figure 1b), was observed within 7 h. To promote the reactivation, an aliquot of hydrazine was added after 85 min. This addition induced a rapid and partial reactivation from 15% to 55% for **15** and from 1% to 40% for **30** in 30 min (Figure 1). Surprisingly, this reactivation did not exceed 65% and 40% for **15** and **30**, respectively. These results suggest the presence of several binding modes in the enzyme–inhibitor complexes.

Mass Spectrometry. The 6-chloromethylcoumarins were designed as mechanism-based inhibitors.⁴⁴ According to their postulated inhibition mechanism (Scheme 3), it is proposed that the lactone carbonyl is first attacked by the nucleophilic Ser195. The subsequent lactone ring opening results in an increase of the leaving properties of the chlorine atom and formation of an electrophilic quinone methide (Scheme 3, pathway a). This latter compound can then form a covalent bond with a nucleophilic residue within the active site. Alternatively, water-mediated deacylation of the acyl enzyme can restore the enzyme activity (Scheme 3, pathway b). Since mass spectrometry is a powerful means to confirm the presence of covalently bound groups in proteins, we measured the mass of the thrombin–inhibitor complexes formed between THR and the two derivatives, **15** and **30**.

The enzyme–inhibitor complexes were produced by portionwise addition of **15** or **30** to THR until an 85% (**15**) or 95% (**30**) inactivation level was reached. An

Table 4. Kinetic Parameters k_i and K_I for Inactivation of THR, FXa, and Trypsin (TRY) by Ester Derivatives **15**, **18**, **23**, **24**, and **30**^a

compd	R	THR ^b k_i/K_I (M ⁻¹ s ⁻¹)	FXa $k_{obs}/[I]$ (M ⁻¹ s ⁻¹)	trypsin $k_{obs}/[I]$ (M ⁻¹ s ⁻¹)	selectivity	
					THR/FXa	THR/TRY
30	2,5-dichlorophenyl	37000 (0.016 min ⁻¹ , 0.424 μM)	220	685	168	54
24	<i>m</i> -bromophenyl	10540 (0.010 min ⁻¹ , 0.983 μM)	430	190	25	55
15	<i>m</i> -chlorophenyl	7720 (0.014 min ⁻¹ , 1.865 μM)	620	310	12	25
23	<i>m</i> -fluorophenyl	2970 (0.006 min ⁻¹ , 2.002 μM)	nd	nd		
18	<i>m</i> -iodophenyl	1210 ^c	nd	nd		

^a nd: not determined. Standard errors are less than 20%. ^b In parentheses: k_i (min⁻¹) and K_I (μM). ^c k_i and K_I were not determined because of weak inhibitory potency for **18**.

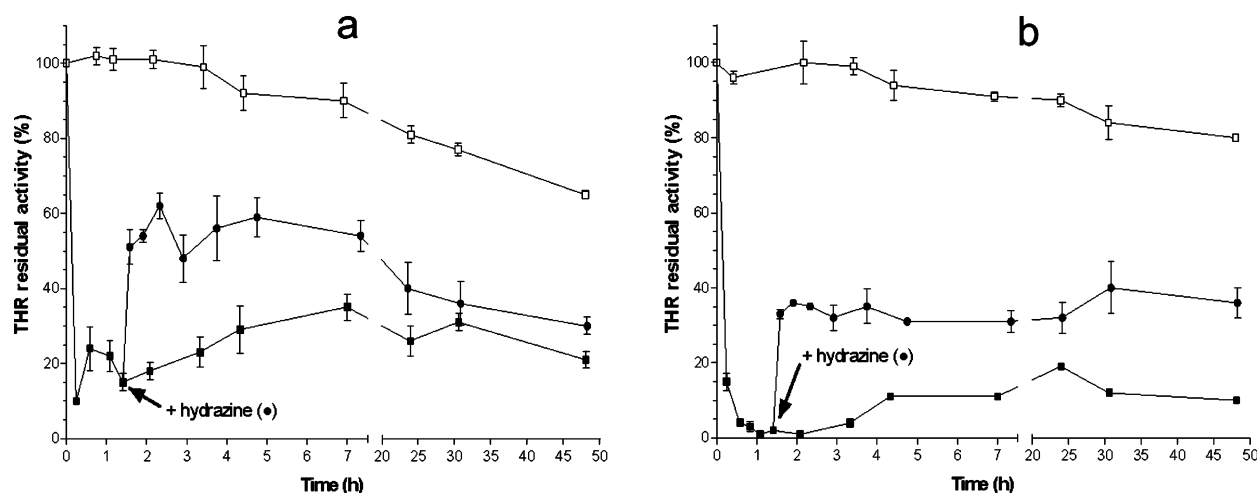
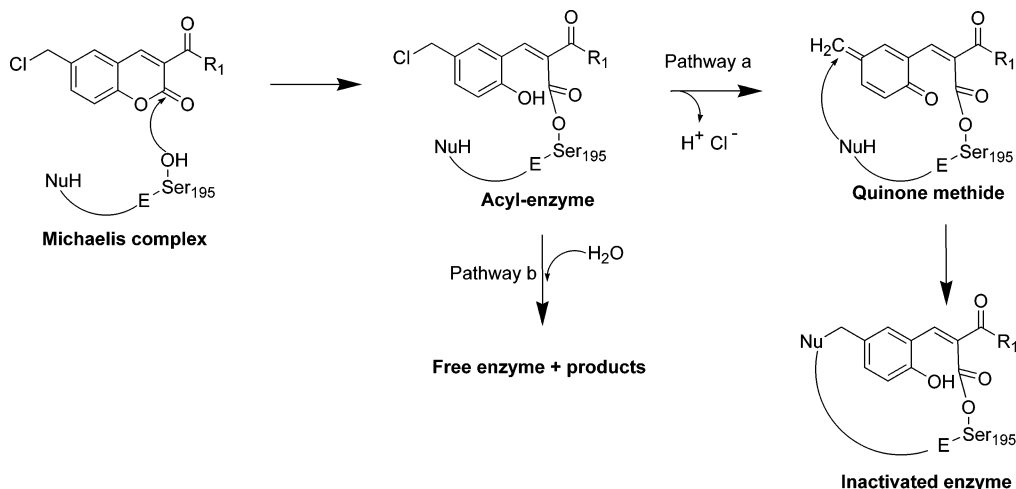


Figure 1. THR enzymatic activity (52.2 nM) after incubation: (a) without (□) or with **15** (10 μM) spontaneous evolution (■), spontaneous evolution followed by hydrazine (0.6 M) addition after 85 min incubation (●); (b) without (□) or with **30** (10 μM) spontaneous evolution (■), spontaneous evolution followed by hydrazine (0.6 M) addition after 85 min incubation (●). Results are expressed as the mean ± SE, $n = 3$.

Scheme 3



aliquot of each complex was then treated with hydrazine (0.6 M) during 1 h. The masses of the native THR and of the different complexes were obtained by LC/MS (Table 5).

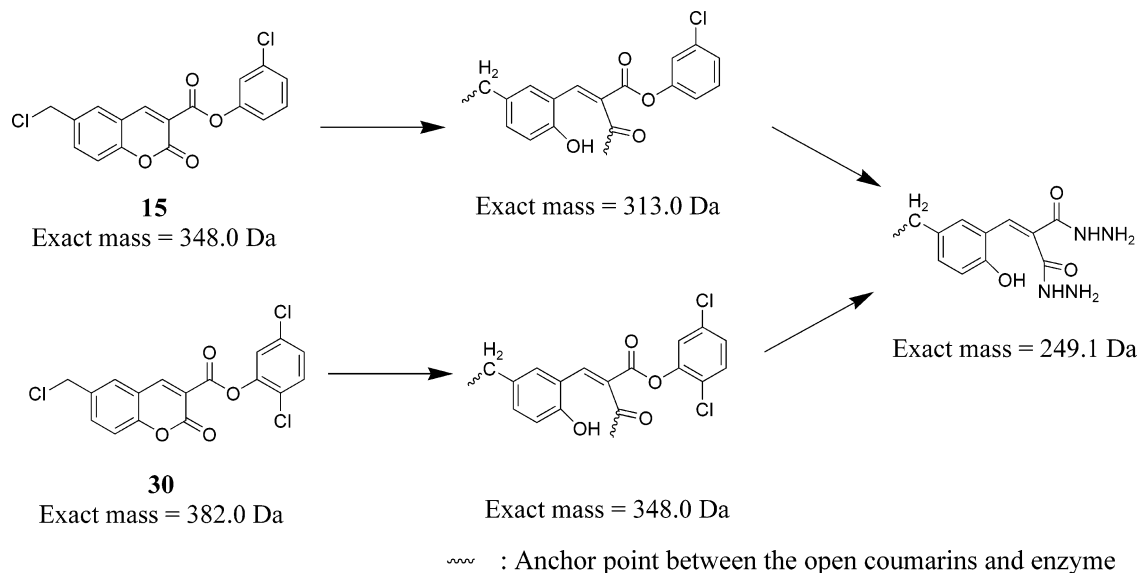
For both inhibitors (**15** and **30**), the mass shift observed between the native THR and the THR–

inhibitor complex corresponds to their exact mass (348.0 and 382.0 Da for **15** and **30**, respectively) less one chlorine atom (exact mass = 313.0 Da and 348.0 for **15** and **30**, respectively) (Scheme 4). These results exclude the formation of a stable acyl enzyme in which Ser195 would have attacked the exocyclic ester (not shown on

Table 5. Observed Mass of Native THR and Enzyme–Inhibitor Complexes

	native THR	THR– 15	THR– 15 treated with hydrazine	THR– 30	THR– 30 treated with hydrazine
mass (Da)	36036.2	36349.4	36036.2 36285.9	36384.0	36036.2 36285.1
Δ mass between complex and native THR ^a (Da)		313.2	0.0 249.7	347.8	0.0 248.9

^a Mass shifts were calculated using the mixture between the complex and the native THR.

Scheme 4

Scheme 3). Treatment of these complexes with hydrazine leads to two entities possessing the same masses whatever the chosen inhibitor, **15** or **30** (Table 5). The lowest one (36 036.2 Da) corresponds to the native THR, explaining the partial reactivation of the enzyme. The second one (36 285.9 and 36 285.1 Da) presents a positive mass shift of 249.7 and 248.9 Da for **15** and **30**, respectively. This shift could be explained by the formation of a dihydrazide complex that would result from a nucleophilic attack of hydrazine on the lactone ring and on the exocyclic ester (Scheme 4).

In comparison with α -CT, the inhibition mechanism starts the same way. In each case, we observed the leaving of the chlorine atom, probably resulting from the opening of the lactone. However, with α -CT, no reactivation was observed, even after treatment with hydrazine.⁴⁴ Moreover, the acyl enzyme complex formed between α -CT and **42**, devoid of any leaving group, is irreversible. These results suggest the formation of a strong interaction between α -CT and **42**, and it can be hypothesized that the acyl function, deeply buried in the binding pocket, cannot be attacked by hydrazine. On the opposite, with THR, we observed a partial induced reactivation that suggests the existence of two binding modes. The first one would be responsible for the irreversible inactivation of THR probably through the formation of a stable alkyl enzyme complex. In the second one, an acyl enzyme could be slowly deacetylated.

Molecular Modeling. In an attempt to support reactivation and mass spectrometry data and to rationalize the trends observed in the enzymatic assays, the molecular interactions between two of the more potent derivatives, **15** and **30**, and the THR active site were investigated. First, binding modes were explored using

the automated GOLD docking program.⁴⁷ The enzyme–inhibitor complexes were then refined by molecular mechanics (DISCOVER3⁴⁸ module from INSIGHTII,⁴⁹ CVFF force field), allowing the active site's side chains to accommodate the ligand.

The study revealed that compounds **15** and **30** interact in a similar manner within the thrombin active site (Figure 2). Their aryl side chain is deeply buried in the specificity binding pocket (S pocket), while the chloromethyl group fits the proximal pocket (P pocket). The distal pocket (D pocket) is left empty. In this bound conformation, both carbonyl moieties of the inhibitors adopt a syn conformation. This is in correlation with the results from a previous structural study⁴³ showing that the syn orientation of the exo carbonyl function versus the lactone in coumarinic derivatives is optimal for the inhibition of α -CT.

Key interactions stabilize both compounds in the binding cleft. A strong hydrogen bond involves the exocyclic carbonyl moiety and the hydroxyl group of Ser195. The coumarin ring favorably interacts through π – π interactions (stacking and CH– π interactions) with the aromatic residues delimiting the P pocket, namely, Tyr60A and Trp60D. Furthermore, an interesting lipophilic contact is observed between Tyr228 located on the back wall of the S binding pocket and the chlorine atom in the meta position in **15** and in the 5-position in **30**. This type of interaction has already been described by the group of Vacca.³¹ This group showed the potent driving nature of such an interaction for thrombin inhibitors with nonbasic P-1 substructures.

The global interaction energy of the complexes formed between THR and **15** and **30** is -36.5 and -37.5 kcal mol⁻¹, respectively. On the basis of these energies, it is

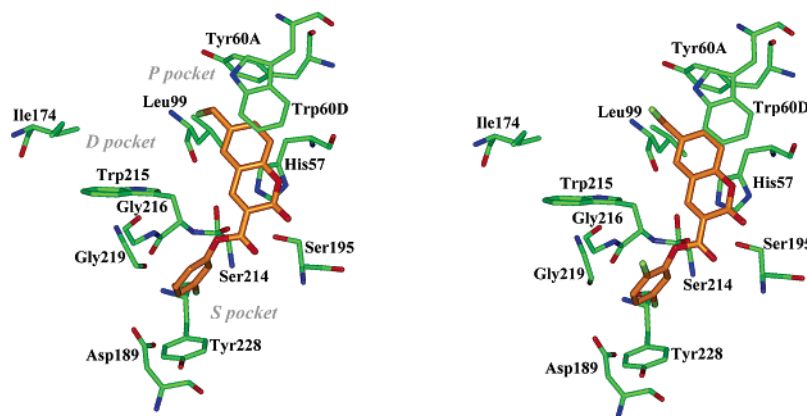


Figure 2. Docking of compounds **15** (left) and **30** (right) into the active site of THR.

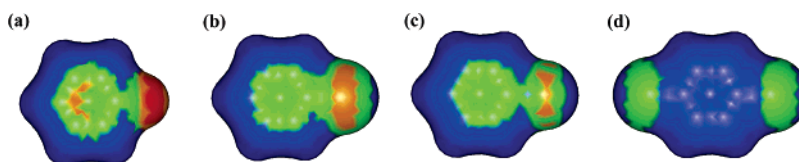


Figure 3. Molecular electrostatic potential (MEP) mapped onto the Connolly surface of (a) fluorophenyl, (b) bromophenyl, (c) chlorophenyl, and (d) 2,5-dichlorophenyl moieties of **23**, **24**, **15**, **30**, respectively. The potentials are shown with identical chromatic scales (red is more negative, greater electron density; blue is more positive, less electron density).

difficult to explain the difference in activity observed in the biological results. Therefore, to estimate the molecular parameters that could influence the affinity of both compounds, the molecular electrostatic potential (MEP) was calculated for the part differing among the two inhibitors, i.e., the *m*-chlorophenyl of **15** and 2,5-dichlorophenyl of **30**, and compared to those of *m*-fluoro- and *m*-bromophenyl of **23** and **24**, respectively (Figure 3). Analysis of the MEP profiles correlates the trends observed in the biological results (reported in Table 4). Indeed, the compounds can be separated into three groups. The fluorophenyl, which corresponds to the lesser active derivative (**23**), exhibits the most electron-rich aromatic ring. In contrast, in the 2,5-dichlorophenyl, which corresponds to the most active derivative (**30**), the surface above the aromatic ring is much less attractive (weaker electron density). The chlorophenyl (**15**) and bromophenyl (**24**) present similar MEP profiles and inhibitory potency, between the two others.

On the basis of these observations, the 2,5-dichlorophenyl of **30** is thought to be much more stabilized in the S pocket, in the vicinity of negatively charged Asp189, than the *m*-chlorophenyl of **15** (the distance between the carboxylate of Asp189 and the centroid of the two rings is 4.6–4.7 Å). This could, in part, explain the difference in activity of **15** vs **30**.

Finally, in each complex, the lactone carbonyl is in proximity to the hydroxyl moiety of the catalytic Ser195. For each case, a distance of 3.2 Å between the carbon of the lactone and the oxygen atom of Ser195 is consistent with the nucleophilic attack of this residue on the coumarin lactone, leading to the acyl enzyme. This result corroborates the postulated inhibition mechanism presented above, as well as the existence of a reversible complex shown in the reactivation study (Figure 1, Scheme 3). Furthermore, in the surrounding of the chloromethyl moiety of the ligand, two amino acid residues (Tyr60A and His57) were identified as potential nucleophilic residues. These should be able to attack the

quinone methide formed after the departure of the chlorine atom (Scheme 3, pathway a), leading to the irreversible complex (alkylated enzyme) revealed by the reactivation study (Figure 1).

Predicted Cell Permeability. Since the final goal in the development of new antithrombotics is bioavailability, we estimated cell permeation using a computational approach for compounds **15**, **18**, **23**, **24**, **30** and compared them with argatroban. For each compound, a set of 94 molecular determinants relevant to the process of membrane partitioning were computed with the VOLSURF software^{50–52} and projected onto a predictive model of Caco2 permeation (Figure 4a). This model, which was developed elsewhere,⁵³ correlates the 94 molecular descriptors with the experimentally obtained permeation of nearly 750 chemically diverse compounds. Derivatives computed to have a value greater than 0.4 are predicted to cross the cell membrane, whereas those with a value lower than –0.4 will have a highly reduced probability of penetrating the Caco2 cell by passive diffusion.

In this model, **15**, **18**, **23**, **24**, and **30** were predicted to behave as very good Caco2 penetrating agents with values of 0.96, 1.03, 0.72, and 1.03, respectively. Argatroban, in contrast, possessed a value of –0.3, which is in agreement with its known poor bioavailability.

For **30**, the influence of individual molecular determinants on the partitioning behavior was analyzed and compared with argatroban. Figure 4b plots the variable weight profile for the Caco2 model. The vertical bars represent the relative contribution of each individual molecular descriptor to the global Caco2 score. Positive bars indicate descriptors whose values are directly proportional to membrane permeability, while descriptors with negative bars show an inverse correlation with permeation. It appears from this plot that the enhancement of Caco2 permeability is mainly due to an increase of compound's hydrophilic integrity moment (*I_w*, which represents the offset between the barycenter of the

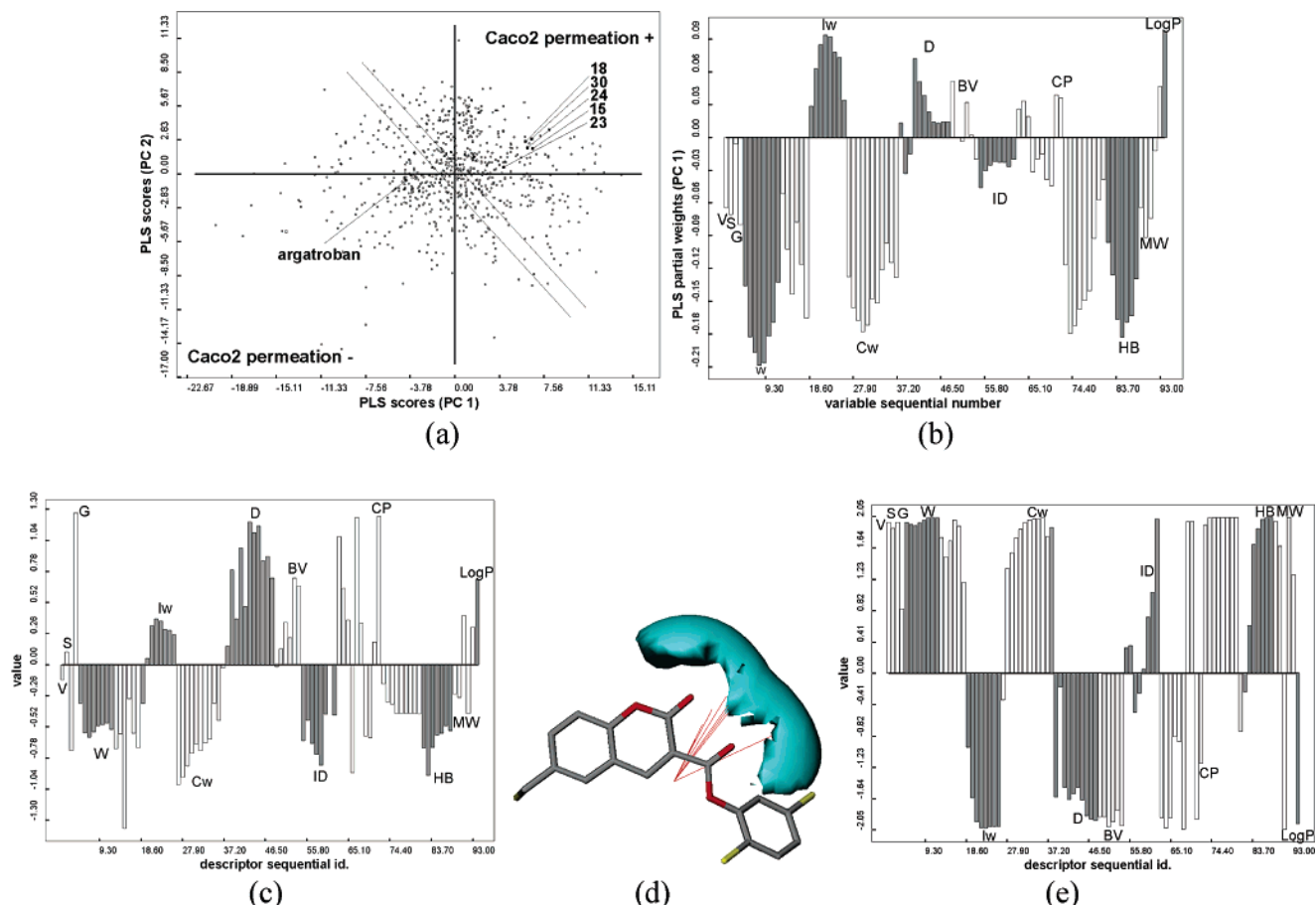


Figure 4. (a) Projection of Caco2 PLS scores of **15**, **18**, **23**, **24**, **30**, and argatroban on Caco2 PLS scores of compounds with known properties. (b) PLS weights profile for VOLSURF descriptors of the Caco2 model: V, volume; S, molecular surface; G, molecular globularity; W, hydrophilic regions; Iw, hydrophilic integrity moment; Cw, capacity factor; D, hydrophobic regions; BV, best volumes; ID, hydrophobic integrity moment; CP, critical packing parameter; HB, hydrogen-bonding; MW, molecular weight. (c) Profile of molecular descriptors computed for **30**. (d) Hydrophilic molecular interaction field (MIF) of **30** calculated with a water probe, represented at -3 kcal/mol. Red vectors correspond to the hydrophilic integrity moments Iw. (e) Profile of molecular descriptors computed for argatroban.

hydrophilic regions and the center of mass of the molecule), hydrophobic regions (D), and $\log P$. On the other hand, descriptors of hydrophilic regions (W), hydrophilic capacity factor (Cw), and H-bonding (HB) are inversely correlated with Caco2 permeability.

Parts c and e of Figure 4 shows the profile of these molecular descriptors computed for **30** and argatroban, respectively. The good predicted permeability of **30** can be notably explained by the combined effects of (i) the presence of a localized hydrophilic region around the two carbonyl moieties (W, Figure 4c,d), which provides an anisotropy of distribution of hydrophilic regions along the molecular axis of **30** (Iw, Figure 4c,d), (ii) the hydrophobic nature of the coumarin ring (D, Figure 4d), and (iii) the absence of H-bond interaction. Conversely, the profile of molecular descriptors for argatroban (Figure 4e) shows that the highly hydrophilic nature (W, Cw, Figure 4d) with H-bonding interaction and low $\log P$ value highly contributes to the poor cell permeability of this compound.

Conclusion

In this work, we evaluated the activity of coumarin-type derivatives as direct inhibitors of THR and FXa. A first screening at 2 and 5 μM for THR and FXa, respectively, highlighted several compounds as strong

inhibitors of THR. Their kinetic parameters k_i/K_i were determined, and it appeared that the most potent compounds on THR were characterized by a 2,5-dichlorophenyl or a 3-halogenophenylester on the 3-position and a chloromethyl function on the 6-position. Moreover, the best inhibitor in this series, **30**, possessed good selectivity over THR because FXa inactivation ($k_{\text{obs}}/[I] = 220 \text{ M}^{-1} \text{ s}^{-1}$) and TRY inactivation ($k_{\text{obs}}/[I] = 685 \text{ M}^{-1} \text{ s}^{-1}$) were 168- and 54-fold lower than the THR one ($k_i/K_i = 37\,000 \text{ M}^{-1} \text{ s}^{-1}$). This study did not allow us to obtain highly potent FXa inhibitors because the best compound (**15**) inhibited FXa with a $k_{\text{obs}}/[I]$ of $620 \text{ M}^{-1} \text{ s}^{-1}$.

The inhibition mechanism toward THR was investigated. Albeit similar results were obtained using compounds **15** and **30** as inhibitors, they significantly differ from that described previously with $\alpha\text{-CT}$. Although the leaving of the chlorine atom was observed with both enzymes, we showed hydrazine-induced partial reactivations for THR. These results were confirmed by LC/MS, which showed the resurgence of the native THR and a new dihydrazide complex. To support these assumptions, a docking study of **15** and **30** within THR was performed. Key interactions (H-bonds, stacking, and lipophilic contacts) stabilizing the compounds in the active site of THR were highlighted. Moreover, com-

parison of the molecular electrostatic potential (MEP) generated around the substituted aryl side chain of inhibitors helped to rationalize the trends observed in the enzymatic assays. This study also showed that the favored conformation and orientation of the inhibitors within THR allow the formation of either an acyl enzyme or an alkyl enzyme and thus corroborate the partially reversible character of the THR inactivation process in this series.

Finally, we have estimated the cell permeability of our derivatives using a computational approach. Generally, our compounds should present very good membrane permeation compared with argatroban, a known THR inhibitor. Nevertheless, the method used here is theoretical and parameters other than cell penetration such as first-pass metabolism should be taken into account when evaluating the bioavailability of coumarins that possess a lactone and a phenyl ester vulnerable to esterase-catalyzed hydrolysis.

Experimental Section

Chemistry. ^1H NMR spectra were performed on Bruker AW 80 (80 MHz) or JEOL JNM EX 400 (400 MHz). The spectra were measured in CDCl_3 with TMS as an internal standard (δ : 0.00 ppm). IR data reported in cm^{-1} were obtained using a BIO-RAD FTS 165 spectrophotometer. Melting points were determined with a Büchi-Tottoli apparatus (B540) in open capillary tubes and are uncorrected. Analyses (C, H, N) were performed on a ThermoFinnigan flash EA 112 analyzer and were within $\pm 0.4\%$ of the theoretical values. Analytical thin-layer chromatography (TLC) experiments were performed on premade, glass-backed plates SiO_2 , 60PF₂₅₄, 250 μm (Merck 5719). Compounds were visualized by UV illumination and by heating to 150 $^\circ\text{C}$ after spraying phosphomolybdic acid in ethanol. All the reactions were performed in two-necked round-bottomed flasks equipped with a septum stopper and an argon-filled balloon. All glassware was warmed prior to use and degassed at 0.1 mmHg. All transfers of reagents were performed via syringes.

General Method for the Synthesis of Esters 6–32, Amide 33, and Thioester 34. To a flask containing 1 g (4.54 mmol) of 6-hydroxymethyl-2-oxo-2H-chromene-3-carboxylic acid was added thionyl chloride (10 mL). This solution was stirred and refluxed under an argon atmosphere during 3 h. After cooling, the mixture was evaporated and anhydrous toluene (10 mL) was added to the residue and evaporated. This operation was repeated three times. Then, to the dried acyl chloride dissolved in dry dioxane (20 mL) was added the required alcohol, thiol, or amine (1.1 equiv) dissolved in anhydrous dioxane (5 mL) and dry pyridine (1.1 equiv). After 2 h, the solvents were evaporated and the residue was dissolved in AcOEt (150 mL) and washed three times with 0.1 N HCl (50 mL). The combined organic phases were dried over MgSO_4 and evaporated to dryness. The products were crystallized in AcOEt/petroleine (40–60 $^\circ\text{C}$).

This method allowed us to obtain derivatives **6–9**, **14–34**, **42–44**, which displayed structural features in agreement with literature.^{36–38}

3-Naphth-1-yl-6-chloromethyl-2-oxo-2H-1-benzopyran-3-carboxylate (10). This was prepared according to the general procedure presented above. Yield: 25%. Mp: 143–146 $^\circ\text{C}$. IR (KBr): 3054 (C–H arom), 1746 (C=O ester), 1713 (C=O lactone), 1622, 1574, 1239, 1222. ^1H NMR (80 MHz, CDCl_3): δ 8.75 (s, 1H), 8.20–7.80 (m, 10H), 4.60 (s, 2H). Anal. ($\text{C}_{21}\text{H}_{13}\text{ClO}_4$) C, H.

3-Naphth-2-yl-6-chloromethyl-2-oxo-2H-1-benzopyran-3-carboxylate (11). This was prepared according to the general procedure presented above. Yield: 30%. Mp: 187–190 $^\circ\text{C}$. IR (KBr): 3054 (C–H arom), 1777 (C=O ester), 1734 (C=O lactone), 1624, 1578, 1247, 1240, 1223. ^1H NMR (80

MHz, CDCl_3): δ 8.70 (s, 1H), 8.00–7.35 (m, 9H), 7.30 (d, 1H), 4.60 (s, 2H). Anal. ($\text{C}_{21}\text{H}_{13}\text{ClO}_4$) C, H

3-Quinol-6-yl-6-chloromethyl-2-oxo-2H-1-benzopyran-3-carboxylate (12). This was prepared according to the general procedure presented above. Yield: 32%. Mp: 205–206 $^\circ\text{C}$. IR (KBr): 3056 (C–H arom), 1771 (C=O ester), 1729 (C=O lactone), 1620, 1575, 1501, 1376, 1294, 1246, 1225, 1210. ^1H NMR (80 MHz, CDCl_3): δ 9.00–8.95 (m, 2H), 8.79 (s, 1H), 8.21–8.18 (m, 2H), 7.80–7.40 (m, 5H), 4.70 (s, 2H). Anal. ($\text{C}_{20}\text{H}_{12}\text{NClO}_4$) H, N. C: calcd 65.67; found 64.64

3-Quinol-8-yl-6-chloromethyl-2-oxo-2H-1-benzopyran-3-carboxylate (13). This was prepared according to the general procedure presented above. Yield: 80%. Mp: 127 $^\circ\text{C}$ (dec). IR (KBr): 3058 (C–H arom), 1770 (C=O ester), 1733 (C=O lactone), 1622, 1575, 1372, 1246, 1214. ^1H NMR (80 MHz, CDCl_3): δ 9.00 (s, 1H), 8.95–8.90 (m, 1H), 8.25–8.17 (m, 1H), 7.80–7.40 (m, 7H), 4.70 (s, 2H). Anal. ($\text{C}_{20}\text{H}_{12}\text{NClO}_4$) C, H, N.

4-(3-Chlorophenyl)-3-oxobutyric Acid Ethyl Ester (37). To a flask containing 4.01 g (23.5 mmol) of 3-chlorophenylacetic acid **35** was added thionyl chloride (20 mL). This solution was stirred and refluxed under an argon atmosphere during 2 h. After cooling, the mixture was evaporated and anhydrous toluene (20 mL) was added to the residue and evaporated. This operation is repeated three times. The acyl chloride was then dissolved in dry CH_2Cl_2 (20 mL) and added via syringe to an ice-cooled solution containing 3.72 g (25.8 mmol) of Meldrum's acid and 47.0 mmol of dry pyridine dissolved in dry CH_2Cl_2 (20 mL). The mixture was stirred under an argon atmosphere and allowed to warm at room temperature during 2 h. The resulting orange solution was then diluted with CH_2Cl_2 (50 mL) and carefully poured onto 2 M HCl and ice (150 mL). The phases were separated, and the aqueous phase was extracted twice with methylene chloride (2×50 mL). The combined organic phases were washed with 1 M HCl (100 mL) and brine (100 mL), dried over MgSO_4 , and evaporated. The resulting orange crystals, which mainly consisted of the acetylated Meldrum's acid, were dissolved in EtOH (50 mL) and refluxed for 3 h. The solvent was removed under reduced pressure and furnished 3.01 g (13.4 mmol) of the desired product as a clear oil. Yield: 57%. ^1H NMR (CDCl_3): δ 7.30–7.26 (m, 3H), 7.11 (m, 1H), 4.20 (q, $J = 7.2$ Hz, 2H), 3.84 (s, 1H), 3.48 (s, 1H), 1.28 (t, $J = 7.2$ Hz, 3H)

3-(3-Chlorobenzoyl)-6-hydroxymethyl-2-oxo-2H-1-benzopyran-2-one (38). This compound was prepared according to the general procedure presented above and used in the next step in a one-pot procedure without any further purification.

3-(3-Chlorobenzoyl)-6-chloromethyl-2-oxo-2H-1-benzopyran-2-one (40). To a flask containing 0.1 g of **38** was added 1 mL of thionyl chloride. This solution was stirred and refluxed under an argon atmosphere during 2 h. After cooling, the mixture was evaporated and anhydrous toluene (20 mL) was added to the residue and evaporated to dryness. This operation is repeated three times. The residue was then dissolved in hot acetone. The suspension was filtered off onto a pad of Celite, and the filtrate was evaporated to half the volume. The precipitate was filtered off, giving 63 mg of the desired pure product. Yield: 10% in two steps. Mp: 198–200 $^\circ\text{C}$. ^1H NMR (CDCl_3): δ 8.12 (s, 1H), 7.85 (s, 1H), 7.75–7.66 (m, 3H), 7.60 (d, 1H), 7.44 (m, 2H), 4.67 (s, 2H). Anal. ($\text{C}_{17}\text{H}_{10}\text{Cl}_2\text{O}_3$) C, H.

3-[2-(3-Chlorophenyl)acetyl]-6-hydroxymethyl-2-oxo-2H-1-benzopyran-2-one (39). This was prepared according to the general procedure presented above. Yield: 26%. Mp: 139–140 $^\circ\text{C}$. ^1H NMR (CDCl_3): δ 8.52 (s, 1H), 7.68–7.66 (m, 2H), 7.38 (d, $J = 8.8$ Hz, 1H), 7.29–7.23 (m, 3H), 7.18 (d, $J = 6.8$ Hz, 1H), 4.79 (d, $J = 4.4$ Hz, 1H), 4.47 (s, 1H), 1.95 (s, 1H). Anal. ($\text{C}_{18}\text{H}_{13}\text{ClO}_4$) H. C: calcd 65.76; found 65.11.

3-[2-(3-Chlorophenyl)acetyl]-6-chloromethyl-2H-1-benzopyran-2-one (41). To a flask containing 559 mg of triphenylphosphine (2.13 mmol) and 483 mg of 2,3-dichloro-5,6-dicyanobenzquinone (2.13 mmol) dissolved in anhydrous methylene chloride (10 mL) was added 831 mg of tetrahexylammonium chloride (2.13 mmol) with stirring at room temperature under an argon atmosphere. Then, an amount of 500

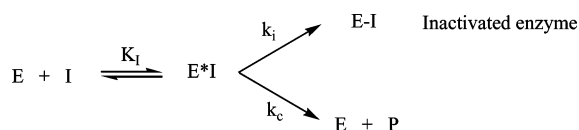
mg of **39** (1.52 mmol) dissolved in anhydrous methylene chloride (15 mL) was added, and the mixture was vigorously stirred. The yellow color immediately changed to deep red. The solution was diluted with CH_2Cl_2 (10 mL) and washed twice with water and once with brine. The combined organic phases were dried over MgSO_4 and evaporated to dryness. Finally, AcOEt (10 mL) was added to the residue and the yellowish precipitate filtered off and washed twice with AcOEt (10 mL) to give 100 mg of pure product. Yield: 20%. Mp: 162–166 °C. ^1H NMR (CDCl_3): δ 8.51 (s, 1H), 7.71–7.67 (m, 2H), 7.40 (d, J = 8.4 Hz, 1H), 7.29–7.24 (m, 3H), 7.18 (d, J = 6.8 Hz, 1H), 4.65 (s, 1H), 4.47 (s, 1H). Anal. ($\text{C}_{18}\text{H}_{12}\text{Cl}_2\text{O}_3$) C, H.

Enzymatic Studies. Human THR and bovine TRY were purchased from Roche, and human FXa was purchased from Kordia. The proteases were assayed spectrophotometrically using *p*-nitroanilide substrates: D-phenylalanylpeptidylarginyl-*p*-nitroanilide (S-2238 from Chromogenix) and tosylglycylprolylarginyl-*p*-nitroanilide (Chromozym TH from Roche) for THR, *N*-methoxycarbonyl-D-norleucylglycyl-L-arginyl-*p*-nitroanilide for FXa (Chromozym X from Roche), and *N*- α -benzoyl-DL-arginyl-*p*-nitroanilide (B4875 from Sigma) for TRY. The reactions were performed in 0.01 M Tris-HCl, 0.01 M HEPES, 0.1 M NaCl, 0.1% (w/v) PEG 6000 and at pH 7.4 for THR, 0.05 M Tris-HCl, 0.15 M NaCl, 0.005 M CaCl_2 , 0.001 M EDTA, 0.05% (v/v) Tween-20 and at pH 7.4 for FXa, and 0.1 M Tris-HCl, 0.01 M CaCl_2 and at pH 8.0 for TRY. Assays contained 10% (v/v) DMSO and were run at 25 °C in a Lambda 20 (Perkin-Elmer) spectrophotometer equipped with a thermostated cell holder. Argatroban was purchased from Sequoia Research Products.

Screening Test. Inactivation measurement at one inhibitor concentration was performed by incubating the inhibitor and the enzyme at 25 °C for 10 min. Then, the residual activity of the enzyme was measured with the appropriate chromogenic substrate (40 μM of S-2238 for THR and 300 μM of Chromozym X for FXa) and compared to a control (enzyme solution without inhibitor). The residual activity percentage was obtained by dividing the measured residual activity with the control activity. The concentrations of enzymes and inhibitors for the screening test were the following: for THR, $[\text{THR}]_0$ = 2.32 nM, $[\text{I}]$ = 2 μM ; for FXa, $[\text{FXa}]_0$ = 5.8 nM, $[\text{I}]$ = 5 μM .

IC_{50} Determination. The 20 μL of test compound in DMSO (or DMSO alone in the control) and 20 μL of human thrombin (Roche, 23.2 nM) in 140 μL of THR kinetic buffer were incubated for 20 min in a 96-well assay plate. An amount of 20 μL of S-2238 (Chromogenix, 2.5 mM) was then added to the mixture. After 5 min of substrate hydrolysis, the reaction was stopped by the addition of 20 μL of 10% acetic acid and the absorbance at 405 nm was measured in a microplate reader (Bio-Rad). The background absorbance was determined with 20 μL of test compound in DMSO (or DMSO alone in the control) mixed with 180 μL of THR kinetic buffer and 20 μL of 10% acetic acid. All compounds were assayed in triplicate at six concentrations. Percent inhibition at each concentration was calculated from the OD at 405 nm from the experimental and control samples. IC_{50} values were calculated from a sigmoidal dose response nonlinear regression equation using GraphPad prism, version 3.02 (GraphPad Software). The reported IC_{50} values are expressed as the mean \pm SEM.

Kinetic Parameters Determination. Suicide substrate inactivation can be represented by the following minimum scheme:



E and I are the free forms of enzyme and inhibitor, respectively, E^*I is a kinetic chimere of the Michaelis complex and the acyl enzyme, E–I is the inactivated enzyme, and P is the product of hydrolysis of I. The kinetic constants k_i and K_I were determined using the preincubation method or the progress curve method.³⁷ Linear and nonlinear regression fits of the

experimental data to the equations were performed with GraphPad prism, version 3.02 (GraphPad Software). At low inhibitor concentrations, the ratio k_i/K_I was obtained as $k_{\text{obs}}/[\text{I}]$ (preincubation method). For the progress curve method, the experimental conditions were as follows: $[\text{THR}]_0$ = 1.16 nM, $[\text{I}]_0$ = 0.025–10 μM , $[\text{Chromozym TH}]$ = 80 μM , and $[\text{FXa}]_0$ = 1.16 nM, $[\text{I}]_0$ = 0.1–10 μM , $[\text{Chromozym X}]$ = 200 μM . For the preincubation method, the enzymes and inhibitors concentrations were as follows: for FXa, $[\text{FXa}]_0$ = 5.8 nM, $[\text{I}]_0$ = 1–5 μM ; for TRY, $[\text{TRY}]_0$ = 145 nM, $[\text{I}]_0$ = 2.5–10 μM .

Spontaneous and Hydrazine Reactivation. To evaluate the irreversible character of the inhibition, enzyme and inhibitor are incubated until a 75% inactivation was reached. The enzyme–inhibitor complexes were then incubated in the presence or absence of hydrazine for 48 h. Enzyme activity of aliquots was monitored and compared to that of the control. The THR activity of each group was expressed as a percent of control at t_0 . For reactivation studies, the experimental conditions were as follows: $[\text{THR}]_0$ = 52.2 nM, $[\text{I}]$ = 10 μM , and $[\text{hydrazine}]$ = 0.6 M.

Mass Spectrometry. Preparation of Enzyme–Inhibitor Complexes. The enzyme–inhibitor complexes were prepared by portionwise addition of inhibitor until an 85% inactivation was reached. These complexes were then incubated with hydrazine for 1 h. For each condition, enzyme aliquots were taken and analyzed by LC/MS. Note that in this case the THR kinetic buffer does not contain PEG-6000. The experimental conditions for the preparation of the complexes were as follows: $[\text{THR}]_0$ = 1.28 μM , $[\text{15}]$ = 40 μM , $[\text{30}]$ = 10 μM , and $[\text{hydrazine}]$ = 0.6 M.

LC/MS. The molecular mass of the enzyme–inhibitor complexes was obtained by injecting 1 μg of these complexes into an Agilent SB-C18 column, pore size 300 Å, particle size 3.5 μm , 50 mm \times 2 mm i.d. at 25 °C. Solvent A consisted of water with 1% formic acid and solvent B of acetonitrile. The gradient profile for solvent B was 5–80% in 20 min. The flow rate was 500 $\mu\text{L min}^{-1}$. After elution from the column, the sample was ionized by an ESI source of the mass spectrometer. ESI/MS experiments were performed on a Agilent 1100 LC/MSD trap (Agilent Technologies) operating in positive ion mode. Instrumental parameters were as follows: nebulizer pressure 40 psi, auxiliary gas flow 6 L min^{-1} , temperature of auxiliary gas 325 °C, and capillary voltage 4.5 kV.

Molecular Modeling. Molecular modeling studies were carried out using INSIGHTII software,⁴⁹ version 2000, running on a Silicon graphics workstation. The structures of the inhibitors were obtained by means of the BUILDER module and optimized using the CFF91 force field. Docking simulations were performed inside the human THR enzymes (PDB code: 1A4W) with the automated GOLD program.⁴⁷ For each inhibitor, the binding mode with the best fit as well as stereoelectronic matching quality was selected. To take into account protein flexibility, all the complexes were then refined with DISCOVER3.⁴⁸ The minimization process, using the CVFF force field (dielectric constant 1 r), includes two steps: the steepest descent algorithm, reaching a convergence of 10.00 kcal $\text{mol}^{-1} \text{\AA}^{-1}$, followed by the conjugated gradient algorithm to reach a final convergence of 0.01 kcal $\text{mol}^{-1} \text{\AA}^{-1}$.

Quantum chemical calculations were performed using the Gaussian 98 program.⁵⁴ The geometries of the four fragments (fluoro-, bromo-, chloro-, and 1,4-dichlorophenyl) were fully optimized, and the molecular electrostatic potential (MEP) was calculated at the HF/6-31G* level of theory. These were plotted onto the Connolly surface (probe 1.4 Å) using the INSIGHTII software.

Cell Permeability. Prediction of Caco2 cell permeation of **15**, **18**, **23**, **24**, **30**, and argatroban was performed with the VOLSURF algorithm,^{50–52} as implemented in SYBYL, version 7.0. The three-dimensional structures of **15**, **18**, **23**, **24**, **30** were obtained using the INSIGHTII software by means of the BUILDER module and optimized using the CFF91 force field. The three-dimensional structure of argatroban was extracted from the active site of thrombin (PDB code: 1DWC). The three-dimensional molecular interaction field (MIF) was first cal-

culated around the target molecule, using the energy (Lennard-Jones, hydrogen-bonding, and Coulombic electrostatics) of interaction with a molecular probe placed at each node of a regular 3D lattice. A grid resolution of 0.5 Å was employed, and three distinct molecular probes (H₂O, DRY, and carbonyl) were used to evaluate both polar and nonpolar molecular regions. In a subsequent step, VOLSURF transforms the MIF into a set of scalar descriptors and projects their values onto a predictive model of Caco2 cell permeation. This predictive model was developed by correlating the same set of descriptors with the experimental permeation of nearly 750 known drugs, using a cross-validated discriminant partial least-squares procedure.

Acknowledgment. This work was supported in part by the “Fonds Spécial de Recherche” (F.S.R., FUNDP, Namur, Belgium), the “Fonds de la Recherche Scientifique Médicale Belge” (F.R.S.M., Grant No. 3.4570.99), the F.R.I.A. (Bruxelles, Belgium) from which J. de Ruyck is a Research Fellow, and the “Fonds National de la Recherche Scientifique” (F.N.R.S., Bruxelles, Belgium) from which C. Charlier is a Research Fellow.

Supporting Information Available: Microanalytical data for all synthesized compounds not included in the Experimental Section. This material is available free of charge via the Internet at <http://pubs.acs.org>.

References

- Hirsh, J.; Weitz, J. I. New antithrombotic agents. *Lancet* **1999**, *353*, 1431–1436.
- Hirsh, J.; Weitz, J. I. Thrombosis and anticoagulation. *Semin. Hematol.* **1999**, *36*, 118–132.
- Thiagarajan, P.; Wu, K. K. Mechanisms of antithrombotic drugs. *Adv. Pharmacol.* **1999**, *46*, 297–324.
- Dahlback, B. Blood coagulation. *Lancet* **2000**, *355*, 1627–1632.
- Davie, E. W.; Fujikawa, K.; Kisiel, W. The coagulation cascade: initiation, maintenance, and regulation. *Biochemistry* **1991**, *30*, 10363–10370.
- Davie, E. W. Biochemical and molecular aspects of the coagulation cascade. *Thromb. Haemostasis* **1995**, *74*, 1–6.
- Mann, K. G. Biochemistry and physiology of blood coagulation. *Thromb. Haemostasis* **1999**, *82*, 165–174.
- Porcari, A. R.; Chi, L.; Leadley, R. Recent advances in clinical trials of the direct and indirect selective Factor Xa inhibitors. *Expert Opin. Invest. Drugs* **2000**, *9*, 1595–1600.
- Tan, K. T.; Makin, A.; Lip, G. Y. Factor X inhibitors. *Expert Opin. Invest. Drugs* **2003**, *12*, 799–804.
- Gould, W. R.; Leadley, R. J. Recent advances in the discovery and development of direct coagulation factor xa inhibitors. *Curr. Pharm. Des.* **2003**, *9*, 2337–2347.
- Hirsh, J.; Warkentin, T. E.; Shaughnessy, S. G.; Anand, S. S.; Halperin, J. L.; Raschke, R.; Granger, C.; Ohman, E. M.; Dalen, J. E. Heparin and low-molecular-weight heparin: mechanisms of action, pharmacokinetics, dosing, monitoring, efficacy, and safety. *Chest* **2001**, *119*, 64S–94S.
- Hirsh, J.; Dalen, J.; Anderson, D. R.; Poller, L.; Bussey, H.; Ansell, J.; Deykin, D. Oral anticoagulants: mechanism of action, clinical effectiveness, and optimal therapeutic range. *Chest* **2001**, *119*, 8S–21S.
- Vacca, J. P. New advances in the discovery of thrombin and factor Xa inhibitors. *Curr. Opin. Chem. Biol.* **2000**, *4*, 394–400.
- Sanderson, P. E. Anticoagulants: Inhibitors of thrombin and factor Xa. *Annu. Rep. Med. Chem.* **2001**, *36*, 79–88.
- Kikumoto, R.; Tamao, Y.; Tezuka, T.; Tonomura, S.; Hara, H.; Ninomiya, K.; Hijikata, A.; Okamoto, S. Selective inhibition of thrombin by (2R,4R)-4-methyl-1-[N2-[(3-methyl-1,2,3,4-tetrahydro-8-quinolyl) sulfonyl]-l-arginyl]-2-piperidinecarboxylic acid. *Biochemistry* **1984**, *23*, 85–90.
- Sturzebecher, J.; Markwardt, F.; Voigt, B.; Wagner, G.; Walsmann, P. Cyclic amides of N- α -arylsulfonylaminoacylated 4-amidinophenylalanine. Tight binding inhibitors of thrombin. *Thromb. Res.* **1983**, *29*, 635–642.
- Eriksson, U. G.; Renberg, L.; Bredberg, U.; Teger-Nilsson, A. C.; Regardh, C. G. Animal pharmacokinetics of inogatran, a low-molecular-weight thrombin inhibitor with potential use as an antithrombotic drug. *Biopharm. Drug Dispos.* **1998**, *19*, 55–64.
- Eriksson, B. I.; Carlsson, S.; Halvarsson, M.; Risberg, B.; Mattsson, C. Antithrombotic effect of two low molecular weight thrombin inhibitors and a low-molecular weight heparin in a caval vein thrombosis model in the rat. *Thromb. Haemostasis* **1997**, *78*, 1404–1407.
- Hilpert, K.; Ackermann, J.; Banner, D. W.; Gast, A.; Gubernator, K.; Hadvary, P.; Labler, L.; Muller, K.; Schmid, G.; Tschopp, T. B.; et al. Design and synthesis of potent and highly selective thrombin inhibitors. *J. Med. Chem.* **1994**, *37*, 3889–3901.
- Kettner, C.; Shaw, E. D-Phe-Pro-ArgCH₂C1-A selective affinity label for thrombin. *Thromb. Res.* **1979**, *14*, 969–973.
- Bajusz, S.; Szell, E.; Bagdy, D.; Barabas, E.; Horvath, G.; Dioszegi, M.; Fittler, Z.; Szabo, G.; Juhasz, A.; Tomori, E.; et al. Highly active and selective anticoagulants: D-Phe-Pro-Arg-H, a free tripeptide aldehyde prone to spontaneous inactivation, and its stable N-methyl derivative, D-MePhe-Pro-Arg-H. *J. Med. Chem.* **1990**, *33*, 1729–1735.
- Neises, B.; Broersma, R. J.; Tarnus, C.; Piriou, F.; Remy, J. M.; Lintz, C.; Heminger, E. F.; Kutcher, L. W. Synthesis and comparison of tripeptidylfluoroalkane thrombin inhibitors. *Bioorg. Med. Chem.* **1995**, *3*, 1049–1061.
- Iwanowicz, E. J.; Lau, W. F.; Lin, J.; Roberts, D. G.; Seiler, S. M. Retro-binding tripeptide thrombin active-site inhibitors: discovery, synthesis, and molecular modeling. *J. Med. Chem.* **1994**, *37*, 2122–2124.
- Boatman, P. D.; Ogbu, C. O.; Eguchi, M.; Kim, H. O.; Nakanishi, H.; Cao, B.; Shea, J. P.; Kahn, M. Secondary structure peptide mimetics: design, synthesis, and evaluation of beta-strand mimetic thrombin inhibitors. *J. Med. Chem.* **1999**, *42*, 1367–1375.
- Li, M.; Lin, Z.; Johnson, M. E. Structure-based design and synthesis of novel thrombin inhibitors based on phosphinic peptide mimetics. *Bioorg. Med. Chem. Lett.* **1999**, *9*, 1957–1962.
- Kettner, C.; Mersinger, L.; Knabb, R. The selective inhibition of thrombin by peptides of boroarginine. *J. Biol. Chem.* **1990**, *265*, 18289–18297.
- Tamura, S. Y.; Levy, O. E.; Uong, T. H.; Reiner, J. E.; Goldman, E. A.; Ho, J. Z.; Cohen, C. R.; Bergum, P. W.; Nutt, R. F.; Brunck, T. K.; Semple, J. E. Guanypiperidine peptidomimetics: potent and selective bis-cation inhibitors of factor Xa. *Bioorg. Med. Chem. Lett.* **2000**, *10*, 745–749.
- Marlowe, C. K.; Sinha, U.; Gunn, A. C.; Scarborough, R. M. Design, synthesis and structure–activity relationship of a series of arginine aldehyde factor Xa inhibitors. Part 1: structures based on the (D)-Arg-Gly-Arg tripeptide sequence. *Bioorg. Med. Chem. Lett.* **2000**, *10*, 13–16.
- Hara, T.; Yokoyama, A.; Ishihara, H.; Yokoyama, Y.; Nagahara, T.; Iwamoto, M. DX-9065a, a new synthetic, potent anticoagulant and selective inhibitor for factor Xa. *Thromb. Haemostasis* **1994**, *71*, 314–319.
- Adler, M.; Davey, D. D.; Phillips, G. B.; Kim, S. H.; Jancarik, J.; Rumennik, G.; Light, D. R.; Whitlow, M. Preparation, characterization, and the crystal structure of the inhibitor ZK-807834 (CI-1031) complexed with factor Xa. *Biochemistry* **2000**, *39*, 12534–12542.
- Tucker, T. J.; Brady, S. F.; Lumma, W. C.; Lewis, S. D.; Gardell, S. J.; Naylor-Olsen, A. M.; Yan, Y.; Sisko, J. T.; Stauffer, K. J.; Lucas, B. J.; Lynch, J. J.; Cook, J. J.; Stranieri, M. T.; Holahan, M. A.; Lyle, E. A.; Baskin, E. J.; Chen, I. W.; Dancheck, K. B.; Krueger, J. A.; Cooper, C. M.; Vacca, J. P. Design and synthesis of a series of potent and orally bioavailable noncovalent thrombin inhibitors that utilize nonbasic groups in the P1 position. *J. Med. Chem.* **1998**, *41*, 3210–3219.
- Lumma, W. C., Jr.; Witherup, K. M.; Tucker, T. J.; Brady, S. F.; Sisko, J. T.; Naylor-Olsen, A. M.; Lewis, S. D.; Lucas, B. J.; Vacca, J. P. Design of novel, potent, noncovalent inhibitors of thrombin with nonbasic P-1 substructures: rapid structure–activity studies by solid-phase synthesis. *J. Med. Chem.* **1998**, *41*, 1011–1013.
- Scozzafava, A.; Briganti, F.; Supuran, C. T. Protease inhibitors. Part 3. Synthesis of non-basic thrombin inhibitors incorporating pyridinium-sulfanilylguanidine moieties at the P1 site. *Eur. J. Med. Chem.* **1999**, *34*, 939–952.
- Clare, B. W.; Scozzafava, A.; Supuran, C. T. Protease inhibitors, part 13: Specific, weakly basic thrombin inhibitors incorporating sulfonyl dicyandiamide moieties in their structure. *J. Enzyme Inhib.* **2001**, *16*, 1–13.
- Sanderson, P. E.; Stanton, M. G.; Dorsey, B. D.; Lyle, T. A.; McDonough, C.; Sanders, W. M.; Savage, K. L.; Naylor-Olsen, A. M.; Krueger, J. A.; Lewis, S. D.; Lucas, B. J.; Lynch, J. J.; Yan, Y. Azaindoles: moderately basic P1 groups for enhancing the selectivity of thrombin inhibitors. *Bioorg. Med. Chem. Lett.* **2003**, *13*, 795–798.
- Pochet, L.; Doucet, C.; Schynts, M.; Thierry, N.; Boggetto, N.; Pirotte, B.; Jiang, K. Y.; Masereel, B.; de Tullio, P.; Delarge, J.; Reboud-Ravaux, M. Esters and amides of 6-(chloromethyl)-2-oxo-2H-1-benzopyran-3-carboxylic acid as inhibitors of α -chymotrypsin: significance of the “aromatic” nature of the novel ester-type coumarin for strong inhibitory activity. *J. Med. Chem.* **1996**, *39*, 2579–2585.

- (37) Doucet, C.; Pochet, L.; Thierry, N.; Pirotte, B.; Delarge, J.; Reboud-Ravaux, M. 6-Substituted 2-oxo-2H-1-benzopyran-3-carboxylic acid as a core structure for specific inhibitors of human leukocyte elastase. *J. Med. Chem.* **1999**, *42*, 4161–4171.
- (38) Pochet, L.; Doucet, C.; Dive, G.; Wouters, J.; Masereel, B.; Reboud-Ravaux, M.; Pirotte, B. Coumarinic derivatives as mechanism-based inhibitors of alpha-chymotrypsin and human leukocyte elastase. *Bioorg. Med. Chem.* **2000**, *8*, 1489–1501.
- (39) Pochet, L.; Frederick, R.; Masereel, B. Coumarin and isocoumarin as serine protease inhibitors. *Curr. Pharm. Des.* **2004**, *10*, 3781–3796.
- (40) Kam, C. M.; Fujikawa, K.; Powers, J. C. Mechanism-based isocoumarin inhibitors for trypsin and blood coagulation serine proteases: new anticoagulants. *Biochemistry* **1988**, *27*, 2547–2557.
- (41) Kam, C. M.; Kerrigan, J. E.; Plaskon, R. R.; Duffy, E. J.; Lollar, P.; Suddath, F. L.; Powers, J. C. Mechanism-based isocoumarin inhibitors for blood coagulation serine proteases. Effect of the 7-substituent in 7-amino-4-chloro-3-(isothioureidoalkoxy)isocoumarins on inhibitory and anticoagulant potency. *J. Med. Chem.* **1994**, *37*, 1298–1306.
- (42) Iranpoor, N.; Firouzabadi, H.; Aghapour, G.; Vaez Zadeh, A. R. Triphenylphosphine/2,3-dichloro-5,6-dicyanobenzoquinone as a new selective and neutral system for the facile conversion of alcohols, thiols and selenols to alkyl halide in the presence of halide ions. *Tetrahedron* **2002**, *58*, 8689–8693.
- (43) Wouters, J.; Huygens, M.; Pochet, L.; Pirotte, B.; Durand, F.; Masereel, B. Structural approach of the mechanism of inhibition of alpha-chymotrypsin by coumarins. *Bioorg. Chem. Lett.* **2002**, *12*, 1109–1112.
- (44) Pochet, L.; Dieu, M.; Frédérick, R.; Murray, A. M.; Kempen, I.; Pirotte, B.; Masereel, B. Investigation of the inhibition mechanism of coumarins on chymotrypsin by mass spectrometry. *Tetrahedron* **2003**, *59*, 4557–4561.
- (45) Silverman, R. B. Mechanism-based enzyme inactivators. *Methods Enzymol.* **1995**, *249*, 240–283.
- (46) Cheng, Y.; Prusoff, W. H. Relationship between the inhibition constant (K_i) and the concentration of inhibitor which causes 50% inhibition (I₅₀) of an enzymatic reaction. *Biochem. Pharmacol.* **1973**, *22*, 3099–3108.
- (47) Jones, G.; Willett, P.; Glen, R. C.; Leach, A. R.; Taylor, R. Development and validation of a genetic algorithm for flexible docking. *J. Mol. Biol.* **1997**, *267*, 727–748.
- (48) *Discover3*, version 2.98; Accelrys Inc.: San Diego, CA, 1998.
- (49) *InsightII*, version 2000; Accelrys Inc.: San Diego, CA, 2000.
- (50) Cruciani, G.; Pastor, M.; Clementi, S. Handling Information from 3D Grid Maps for QSAR Studies. *Molecular Modeling and Prediction of Bioactivity*; Kluwer Academic/Plenum Publishers: New York, 2000; pp 73–82.
- (51) Cruciani, G.; Crivori, P.; Carrupt, P.-A.; Testa, B. Molecular fields in quantitative structure-permeation relationships: the VolSurf approach. *J. Mol. Struct.: THEOCHEM* **2000**, *503*, 17–30.
- (52) Crivori, P.; Cruciani, G.; Carrupt, P. A.; Testa, B. Predicting blood–brain barrier permeation from three-dimensional molecular structure. *J. Med. Chem.* **2000**, *43*, 2204–2216.
- (53) URL: <http://www.moldiscovery.com>.
- (54) Frisch, M. J.; Trucks, G. W.; Schlegel, H. B.; Scuseria, G. E.; Robb, M. A.; Cheeseman, J. R.; Zakrzewski, V. G.; Montgomery, J. A., Jr.; Stratmann, R. E.; Burant, J. C.; Dapprich, S.; Millam, J. M.; Daniels, A. D.; Kudin, K. N.; Strain, M. C.; Farkas, O.; Tomasi, J.; Barone, V.; Cossi, M.; Cammi, R.; Mennucci, B.; Pomelli, C.; Adamo, C.; Clifford, S.; Ochterski, J.; Petersson, G. A.; Ayala, P. Y.; Cui, Q.; Morokuma, K.; Malick, D. K.; Rabuck, A. D.; Raghavachari, K.; Foresman, J. B.; Cioslowski, J.; Ortiz, J. V.; Stefanov, B. B.; Liu, G.; Liashenko, A.; Piskorz, P.; Komaromi, I.; Gomperts, R.; Martin, R. L.; Fox, D. J.; Keith, T.; Al-Laham, M. A.; Peng, C. Y.; Nanayakkara, A.; Gonzalez, C.; Challacombe, M.; Gill, P. M. W.; Johnson, B. G.; Chen, W.; Wong, M. W.; Andres, J. L.; Head-Gordon, M.; Replogle, E. S.; Pople, J. A. *Gaussian 98*, revision A.11; Gaussian, Inc.: Pittsburgh, PA, 1998.

JM050448G